ChemComm

Accepted Manuscript

Volume 52 | Number 1 | 4 January 2016 | Pages 1–216

ChemComm

Chemical Communications
www.rsc.org/chemcomm

ISSN 1359-7345

ROYAL SOCIETY
OF CHEMISTRY

COMMUNICATION
Marilyn M. Olmstead, Alan L. Balch, Josep M. Poblet, Luis Echegoyen et al.
Reactivity differences of Sc_NbC_2n = 68 and 80. Synthesis of the first methanofullerene derivatives of Sc_NbC_80

175 YEARS

This is an Accepted Manuscript, which has been through the Royal Society of Chemistry peer review process and has been accepted for publication.

Accepted Manuscripts are published online shortly after acceptance, before technical editing, formatting and proof reading. Using this free service, authors can make their results available to the community, in citable form, before we publish the edited article. We will replace this Accepted Manuscript with the edited and formatted Advance Article as soon as it is available.

You can find more information about Accepted Manuscripts in the author guidelines.

Please note that technical editing may introduce minor changes to the text and/or graphics, which may alter content. The journal's standard Terms & Conditions and the ethical guidelines, outlined in our author and reviewer resource centre, still apply. In no event shall the Royal Society of Chemistry be held responsible for any errors or omissions in this Accepted Manuscript or any consequences arising from the use of any information it contains.

ROYAL SOCIETY
OF CHEMISTRY

rsc.li/chemcomm

ChemComm

Journal Name

COMMUNICATION

Distinguishing between homogeneous and heterogeneous hydrogen-evolution catalysis with molecular cobalt complexes

David J. Sconyers[a] and James D. Blakemore[a],*

Molecular proton-reduction catalysts can decompose under the acidic conditions required for hydrogen evolution, resulting in formation of secondary metal-containing materials. Using an electrochemical quartz crystal microbalance (EQCM), we report a new method for probing electrodeposition of catalytically active heterogeneous material from molecular precursors. The data collected suggest that EQCM can provide a direct measure of the homogeneity of molecular proton-reduction catalysts over short timescales.

The development of stable proton-reduction catalysts is key for the assembly of systems capable of storing reducing equivalents as hydrogen fuel.[1,2] Molecular H_2-evolving catalysts have attracted significant attention because they are readily derivatized and can be investigated in solution for mechanistic information.[3,4,5] However, molecular mechanisms can be difficult to elucidate—either a molecular species or secondary heterogeneous material produced *in situ* could catalyze the reaction of interest. A number of methods have been applied to distinguish between these cases.[6,7,8] Electrode-driven catalysis presents special, additional challenges to determining mechanisms—the catalyst is usually in a dilute solution, containing a high concentration of electrolyte, and only a small fraction of material is sufficiently near to the electrode to be active.[9,10]

Cobaloxime complexes are among the most celebrated molecular catalysts for proton reduction.[11,12,13] They have been deployed in diverse electrochemical, photochemical, and photoelectrochemical systems for hydrogen evolution.[14] The bis(difluoroboryl)-substituted complex **1** (Scheme 1) is especially attractive, as it can operate at modest overpotentials.[15,16] The analogous complex with proton bridges (**2**) has also received attention.[17]

However, several groups have found that cobaloximes can be unstable under the electrochemical conditions used to drive catalysis. For example, Artero and co-workers described cobalt metal formation from **1** in aqueous solutions upon reduction.[18] Glyoximes can undergo hydrogenation and decomposition following reduction, as shown by coulometric and spectroscopic methods.[19,20] Decomposition of **1** in the presence of strong acid (e.g., 4-cyanoanilinium, $pK_a = 7$ in MeCN)[21] has also been observed by UV-Vis spectroscopy.[22] In most cases, electrochemical methods and/or *ex situ* spectroscopic investigations were used to understand the observed reactivity.

We now report that an electrochemical quartz crystal microbalance (EQCM) may be used to probe such catalyst decomposition *in situ* during electrode polarization. With this technique, a mass change can be measured due to deposition of material on the electrode surface; in the case of a fully homogeneous catalyst, no such mass changes would be detected. Additionally, the EQCM can provide unique data regarding formation of *transient* heterogeneous material—an important consideration, as conditions for H_2 evolution can be corrosive to materials deposited on the electrode surface.

In order to develop this EQCM technique, we used the strong organic acid protonated dimethylformamide ($[DMFH]^+[OTf]^-$, $pK_a = 6.1$ in MeCN)[23] to understand the chemistry that can give rise to secondary electrodeposition precursors from **1** and **2**. Monitoring of treatment of **1** and **2** with 2 equiv. $DMFH^+$ by infrared spectroscopy revealed the appearance of new signals at 614 cm^{-1} and 3300 cm^{-1}, respectively. The signal at 3300 cm^{-1} is consistent with the O-H stretching vibration of free $dmgH_2$ (see ESI). The absence of this signal in the reaction of **1** with acid suggests that no free $dmgH_2$ is formed in this case.

To explain this difference, we turned to nuclear magnetic resonance spectroscopy (NMR). The ^{11}B NMR spectrum of **1** in CD_3CN shows a single broad resonance, centered at 42 ppm, consistent with its paramagnetic nature ($S = 1/2$). Addition of 3 equiv. of $DMFH^+$ results in attenuation of this broad signal and formation of a new, sharp singlet at 2 ppm. No other signals were present, suggesting formation of a single new

[a.] *Department of Chemistry, University of Kansas, 1251 Wescoe Hall Drive, Lawrence, Kansas 66045, USA.*

diamagnetic compound. By ^{19}F NMR, **1** is NMR silent. Addition of 3 equiv. of DMFH$^+$ results in the appearance of two new signals – a sharp singlet at −152 ppm and a broader signal at −79 ppm. The singlet at −79 ppm is consistent with the triflate counterion of the added acid.

Based on high symmetry in NMR spectra, and the observed unique vibration in the IR spectrum, we propose formation of "free-base" **3** (C_{2v} symmetry) upon strong acid addition.[24] Out-of-plane N-H vibrations in free-base porphyrins have been reported between 690-710 cm^{-1}, similar to the signal observed for the reaction of **1** with DMFH$^+$ (614 cm^{-1}).[25] Integration of the ^{19}F NMR singlet at −152 ppm versus an internal standard (hexafluorobenzene) indicates that ca. 10% of the complex decomposes to form this "free-base" macrocycle **3**.

Protonation of **1** or **2** in MeCN thus appears to generate (dmgBF$_2$)$_2$H$_2$ (**3**) or dmgH$_2$ (**4**), respectively. Mass balance dictates co-generation of a Co(II) species, presumably bearing MeCN ligands. [Co(NCMe)$_6$](BF$_4$)$_2$ (**5**) can be prepared chemically and isolated;[26] the analogous [Co(NCMe)$_6$](OTf)$_2$ (**6**) should be generated *in situ* here. The broadened triflate signal in ^{19}F NMR for **1** treated with DMFH$^+$ (FWHM = 22 vs. 5.5 Hz without cobalt) may result from exchange at paramagnetic Co(II).
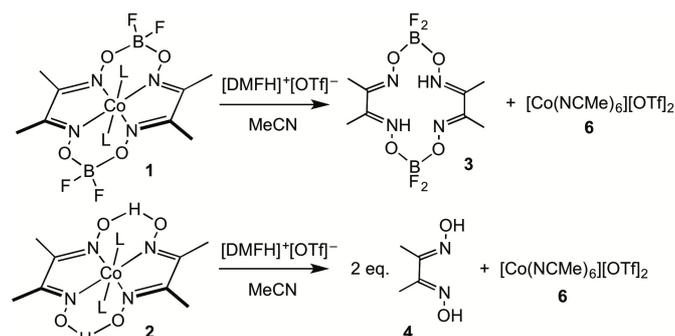


Scheme 1. Reactions of cobaloximes with strong acid DMFH$^+$.

Having observed the reactivity described above, we turned our attention to the electrochemical behavior of the glyoxime complex **1** and solvento species **5**. Cyclic voltammograms collected on a solution of **1** with a graphite working electrode show a virtually reversible one-electron reduction centered at −0.89 V vs. Fc$^{+/0}$ (Figure 1). The peak currents increase linearly with the square root of the scan rate, as expected for a diffusional species. Upon addition of 3 equiv. of DMFH$^+$, the reduction event becomes fully irreversible and the current is enhanced, consistent with H$_2$ evolution catalysis. Noticeably, in these scans, we consistently observe an additional minor reductive feature near −1.3 V, suggesting formation of a new redox-active species upon acid addition.

For a solution of **5**, we observe a single, irreversible reduction with onset near −1.1 V that peaks at −1.3 V.[27] This process is diffusional (see ESI) and virtually irreversible. After excursion to negative potential, an anodic wave appears near +0.3 V (see ESI). The position and shape of this wave are similar to those measured for anodic stripping of cobalt in aqueous solutions.[28] We thus conclude that [Co(NCMe)$_6$]$^{2+}$

undergoes a net two-electron reduction beyond −1.0 V, resulting in formation of metallic cobalt on the electrode. This assignment is confirmed by X-ray photoelectron (XP) spectra collected on carbon electrodes polarized at −1.5 V for 5 minutes, in which distinct cobalt signals are observed (see ESI). Addition of acid to **5** results in a marked enhancement of cathodic current; this current can drive both cobalt deposition and Co metal-catalyzed H$_2$ generation. This agrees well with the relatively positive thermodynamic potential for H$_2$ evolution under these conditions (E^o ≥ −389 mV vs. Fc$^{+/0}$).[23]
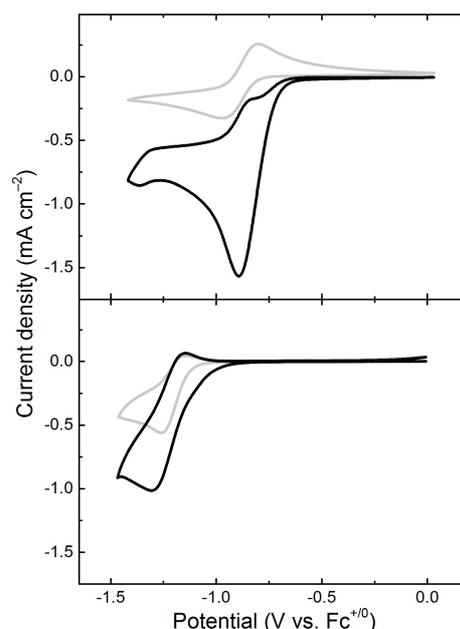
Figure 1. Cyclic voltammograms of solutions containing cobalt complexes. Upper panel: **1** (gray line) and **1** plus 3 equiv. of DMFH$^+$ (black line). Lower panel: **5** (gray line) and **5** plus 3 equiv. of DMFH$^+$ (black line). [Co^{2+}] = 2 mM. (CH$_3$CN, 0.1 M [^{n}Bu$_4$N]$^+$[PF$_6$]$^-$. Working electrode: highly oriented pyrolytic graphite).

In cyclic voltammetry of **1** carried out in the presence of 3 equiv. of DMFH$^+$, no anodic stripping currents are observed, suggesting very little or no cobalt deposition on the electrode (see ESI). This is surprising, as experiments with solutions of **5** always show clear formation of cobalt metal, regardless of the presence of acid.

Thus, we turned to an electrochemical quartz crystal microbalance (EQCM) to provide *real-time* data on cobalt deposition during electrode polarization. EQCM relies on the converse piezoelectric effect to monitor mass changes at the working-electrode surface during an electrochemical experiment.[29] Briefly, if a change in mass or in viscoelastic pressure occurs at the working electrode, the resonant vibration of the electrode shifts in magnitude and sign. The Sauerbrey equation relates the change in frequency to a change in mass, assuming no complicating viscoelastic effects. The EQCM is exceptionally sensitive, and, under the present experimental conditions, can monitor mass changes as small as ±5 ng (frequency units: ±5 Hz; electrode area: 0.205 cm^2). EQCM techniques have been used to measure aqueous deposition and stripping of thin layers of cobalt metal in prior work, encouraging its application here.[30]

ChemComm

EQCM studies on solutions containing $[Co(NCMe)_6](BF_4)_2$ (**5**) confirm cathodic electrodeposition (Figure 2(a)). On the first cathodic scan of a solution containing 2 mM **5** and 3 equiv. of $DMFH^+$, an irreversible current is measured with a peak near –1.25 V. During the return scan to positive potentials, an oxidative stripping process occurs at –0.45 V, consistent with Co^0 oxidation on Au.[30] Mass deposits cathodically beyond –0.8 V, and moving positive of –0.8 V on the anodic sweep results in a rapid drop in mass, consistent with the observed stripping current. Subsequent cycles are comparable; we measure ca. 730 ng of cobalt metal reversibly deposited for each cycle. Similar mass deposits in the absence of acid. (See ESI.)

Based on charge passed in the voltammetry without acid present, the calculated mass deposited (353 ng) agrees well with the predicted mass stripped (356 ng). However the EQCM measures a larger actual mass change (795 ng, see ESI), even in the absence of acid. It is possible that tightly bound or encapsulated solvent may increase the apparent electrode mass (ca. 1.75 MeCN per Co). This is consistent with formation of small cobalt metal "islands" driven by rapid reduction of soluble cobalt. Upon addition of acid, the measured amount of cobalt deposited is similar (730 ng). Thus, reductive current drives both Co deposition and Co-catalyzed H_2 generation.

EQCM experiments carried out on a solution of catalyst **1** in the absence of acid are shown in Figure 2(b). As expected for the pure compound, we observe a single virtually reversible Co(II/I) couple. No significant mass change at the electrode surface is observed during voltammetry. This is consistent with prior chemical work—both the Co(II) and Co(I) forms of **1** are essentially soluble in MeCN.

Upon addition of acid to the solution containing **1** (Figure 2(c)), the usual current response is encountered: loss of reversibility for the Co(II/I) couple and an increase in cathodic current signifying molecular catalysis. The mass data from the EQCM, however, reveal contribution from the behaviour of $[Co(NCMe)_6]^{2+}$ (**6**) generated upon addition of acid. Specifically, near the onset of the pseudo-catalytic current at –0.75 V, we observe a significant mass increase at the electrode surface that continues throughout the cathodic sweep (ca. 50 ng). Immediately preceding this mass increase, a shallow decrease in mass is measured, consistent with formation of hydrogen bubbles at the electrode surface due to catalysis—bubble formation decreases the viscoelastic pressure of the contacting electrolyte medium and registers as an apparent mass decrease.[29] On the return anodic scan, the 50 ng of electrodeposited material is rapidly lost from the surface of the electrode, returning the recorded mass to near its initial value (i.e., Δm ≈ 0 ng).

Notably, use of anilinium triflate as a proton source (pk_a = 10.6 in MeCN)[21] does not result in detectable decomposition of **1** as judged by NMR or IR spectroscopy. EQCM studies of **1** with anilinium triflate do not show mass deposition during electrode polarization (see ESI). These results agree with recent detailed studies of molecular catalysis with **1** and a series of substituted anilinium acids.[22]

The available data therefore suggest that the decomposition pathway of **1** upon treatment with $DMFH^+$ involves formation

of $[Co(NCMe)_6]^{2+}$—this is supported by both spectroscopy and electrochemical findings. The EQCM confirms that cobalt is deposited upon reduction of $[Co(NCMe)_6]^{2+}$, and that deposition does not require presence of acid. In line with these observations, XP spectra collected on electrodes polarized to –1.5 V for 5 min. in solutions containing $[Co(NCMe)_6]^{2+}$ either alone or with acid show signals for cobalt (see ESI).
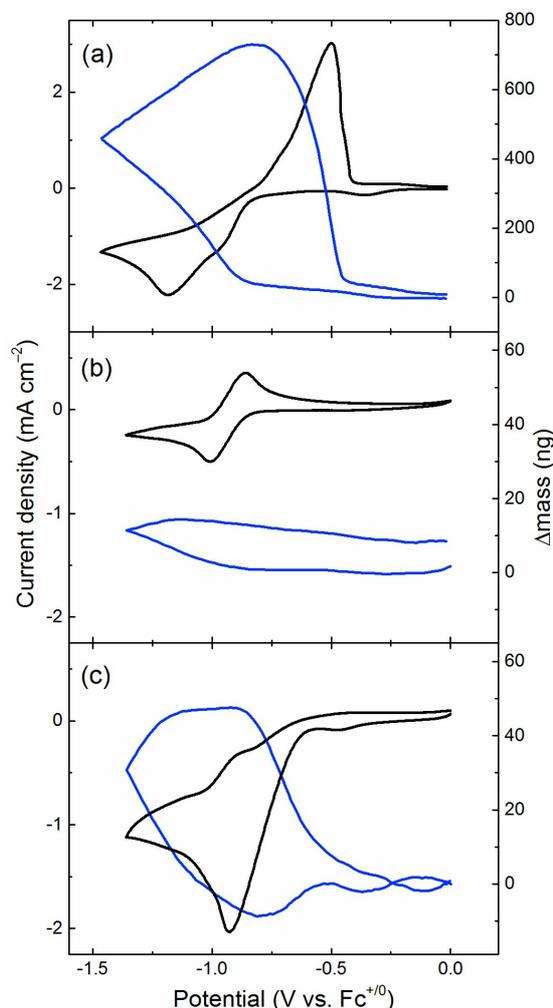
Figure 2. Potential-dependent current (black lines) and mass (blue lines) data for solutions containing (a) **5** and 3 equiv. of $DMFH^+$, (b) **1**, and (c) **1** and 3 equiv. of $DMFH^+$. $[Co^{2+}]$ = 2 mM. (CH_3CN, 0.1 M $[^nBu_4N]^+[PF_6]^-$. Working electrode: gold-coated quartz disk).

However, we were surprised to find that XP spectra collected on electrodes polarized to –1.3 V for 5 min. in the presence of **1** and acid show no cobalt on the surface. Polarization at –0.34 V for 5 min. also gives spectra free of cobalt signals (see ESI). To investigate this, we carried out linear sweep voltammetry using the EQCM on solutions containing **1** and acid (see ESI). The linear cathodic sweep appears as it does in cyclic voltammetry, but allowed us to observe any mass changes that immediately follow the polarization that deposits cobalt metal. A voltage scan from 0 to –1.35 V was carried out, and the instrument was then immediately returned to open circuit, ending the polarization. The mass profile shows a steady readout (Δm ≈ 0) prior to polarization, followed by mass deposition upon excursion beyond –0.94 V, as expected based

ChemComm Accepted Manuscript

COMMUNICATION

on the results described above. However, following the return to open circuit, the mass gained via cobalt deposition (ca. 30 ng) is lost within 10 seconds (see ESI). This is consistent with rapid corrosion of nascent cobalt material on the surface by DMFH$^+$ in solution. This observation agrees with the CV experiment—there is no anodic stripping wave yet mass loss from the surface is detected.

This process, analogous to corrosion of cobalt metal in aqueous solution,[31] should result in hydrogen evolution:

$$Co\ (s) + 2DMFH^+ \rightarrow Co^{2+} + H_2\ (g) + 2DMF$$

To confirm the ability of electrodeposited cobalt to evolve H$_2$ in the presence of DMFH$^+$, we prepared an electrode with a small amount of Co on the surface by reduction of **5**, passing 243 mC during an electrodeposition. Exposure of this electrode to a solution containing 6 mM DMFH$^+$ results in generation of 20 μL of H$_2$, confirming corrosion of cobalt metal under these conditions (see ESI).

The present study showcases the potential of the EQCM technique as a useful method in future studies of proton-reduction catalysis. Formation of heterogeneous material is challenging to detect in electrochemical cells, and our experiments show that such material can even be transient—only present during reductive polarization that cathodically protects against corrosion.[32] This is especially problematic as reductive polarization is required to drive electrocatalysis. However, we note that lack of a mass change does not exclude formation of *soluble* secondary materials by action of acid on catalyst precursors. Nonetheless, considering the challenges in distinguishing between homo- and heterogeneous catalysis, we propose that the EQCM can provide useful real-time information on catalyst stability. Such information could aid in the discovery and development of highly active systems for storing clean energy in chemical fuels.

Acknowledgements

References

1   N. S. Lewis and D. G. Nocera, *Proc. Nat. Acad. Sci. U.S.A.*, 2006, **103**, 15729-15735.

2   M. Rakowski Dubois and D. L. Dubois, *Acc. Chem. Res.*, 2009, **42**, 1974-1982.

3   J. L. Dempsey, J. R. Winkler and H. B. Gray, *J. Am. Chem. Soc.*, 2010, **132**, 16774-16776.

4   D. C. Lacy, G. M. Roberts and J. C. Peters, *J. Am. Chem. Soc.*, 2015, **137**, 4860-4864.

5   J. T. Muckerman and E. Fujita, *Chem. Commun.*, 2011, **47**, 12456-12458.

6   R. H. Crabtree, *Chem. Rev.*, 2015, **115**, 127-150.

7   G. M. Whitesides, M. Hackett, R. L. Brainard, J. Lavalleye, A. F. Sowinski, A. N. Izumi, S. S. Moore, D. W. Brown and E. M. Staudt, *Organometallics*, 1985, **4**, 1819-1830.

8   Y. Lin and R. G. Finke, *Inorg. Chem.*, 1994, **33**, 4891-4910.

9   J. J. Stracke and R. G. Finke, *J. Am. Chem. Soc.*, 2011, **133**, 14872-14875.

10 N. D. Schley, J. D. Blakemore, N. K. Subbaiyan, C. D. Incarvito, F. D'Souza, R. H. Crabtree and G. W. Brudvig, *J. Am. Chem. Soc.*, 2011, **133**, 10473-10481.

11 W. T. Eckenhoff, W. R. McNamara, P. Du and R. Eisenberg, *Biochim. Biophys. Acta, Bioenerg.*, 2013, **1827**, 958-973.

12 G. N. Schrauzer, *Acc. Chem. Res.*, 1968, **1**, 97-103.

13 P. Connolly and J. H. Espenson, *Inorg. Chem.*, 1986, **25**, 2684-2688.

14 L. M. Utschig, S. C. Silver, K. L. Mulfort and D. M. Tiede, *J. Am. Chem. Soc.*, 2011, **133**, 16334-16337.

15 M. Razavet, V. Artero and M. Fontecave, *Inorg. Chem.*, 2005, **44**, 4786-4795.

16 X. L. Hu, B. S. Brunschwig and J. C. Peters, *J. Am. Chem. Soc.*, 2007, **129**, 8988-8998.

17 J. Hawecker, J. M. Lehn and R. Ziessel, *Nouv. J. Chim.*, 1983, **7**, 271-277.

18 S. Cobo, J. Heidkamp, P.-A. Jacques, J. Fize, V. Fourmond, L. Guetaz, B. Jousselme, V. Ivanova, H. Dau, S. Palacin, M. Fontecave and V. Artero, *Nat. Mater.*, 2012, **11**, 802-807.

19 E. Anxolabehere-Mallart, C. Costentin, M. Fournier, S. Nowak, M. Robert and J.-M. Saveant, *J. Am. Chem. Soc.*, 2012, **134**, 6104-6107.

20 E. Anxolabehere-Mallart, C. Costentin, M. Fournier and M. Robert, *J. Phys. Chem. C*, 2014, **118**, 13377-13381.

21 J. T. Muckerman, J. H. Skone, M. Ning and Y. Wasada-Tsutsui, *Biochim. Biophys. Acta, Bioenerg.*, 2013, **1827**, 882-891.

22 E. S. Rountree, D. J. Martin, B. D. McCarthy and J. L. Dempsey, *ACS Catal.*, 2016, **6**, 3326-3335.

23 A. M. Appel and M. L. Helm, *ACS Catalysis*, 2013, **4**, 630-633.

24 Burdinski, F. Birkelbach, M. Gerdan, A. X. Trautwein, K. Wieghardt and P. Chaudhuri, *J. Chem. Soc., Chem. Commun.*, 1995, 963-964.

25 J. O. Alben, S. S. Choi, A. D. Adler and W. S. Caughey, *Ann. N.Y. Acad. Sci.*, 1973, **206**, 278-295.

26 R. A. Heintz, J. A. Smith, P. S. Szalay, A. Weisgerber and K. R. Dunbar, *Inorg. Synth.*, 2002, **33**, 75-83.

27 J. Ke, W. Su, S. M. Howdle, M. W. George, D. Cook, M. Perdjon-Abel, P. N. Bartlett, W. Zhang, F. Cheng, W. Levason, G. Reid, J. Hyde, J. Wilson, D. C. Smith, K. Mallik and P. Sazio, *Proc. Natl. Acad. Sci. USA*, 2009, **106**, 14768-14772.

28 K. Mech, P. Żabiński and R. Kowalik, *J. Electrochem. Soc.*, 2013, **160**, D246-D250.

29 D. A. Buttry and M. D. Ward, *Chem. Rev.*, 1992, **92**, 1355-1379.

30 J. T. Matsushima, F. Trivinho-Strixino and E. C. Pereira, *Electrochim. Acta*, 2006, **51**, 1960-1966.

31 M. Pourbaix, *Lectures on Electrochemical Corrosion*, Plenum Press, 1973.

32 J. Morgan, *Cathodic Protection*, NACE International, 2nd edn., 1987.